

Ion compositions and energies in inductively coupled plasmas generated in low global-warming-potential gases

A N Goyette[†], Yicheng Wang[‡] and J K Olthoff

Electricity Division
Electronics and Electrical Engineering Laboratory
National Institute of Standards and Technology
Gaithersburg, MD 20899-8113

Abstract. Many high density discharges used in microelectronics fabrication use fluorocarbon gases with coincidentally high global-warming potentials (GWPs). We have determined the identities, fluxes, and energy distributions of ions produced in high density discharges generated in two low GWP gases, CF_3I and $\text{CF}_3\text{CH}_2\text{F}$ (HFC-134a), which have attracted interest for plasma processing applications. Measurements were made using a combined ion energy analyser-mass spectrometer that samples ions through an orifice in the lower electrode of an inductively coupled Gaseous Electronics Conference (GEC) rf reference cell. The effects of plasma operating conditions and Ar dilution on ion fluxes and energies were examined. Nearly complete dissociation of CF_3I occurs in CF_3I discharges and I^+ comprises almost all of the ion yield. Mean ion energies range from 5 eV to 10 eV for the operating conditions investigated. Discharges generated in mixtures of CF_3I with Ar have ion fluxes and energies resembling those in pure CF_3I discharges. Pure HFC-134a discharges produce several ions of significant intensity, with HF^+ and Si^+ being the most abundant. Mean ion energies range from 20 eV to 35 eV, and decrease as HFC-134a is diluted with Ar. Higher discharge powers result in greater dissociation in HFC-134a discharges, shifting the ion composition towards higher fluxes of lighter ions.

PACS numbers: 52.70.Nc, 52.75.Rx

[†] Electronic mail: goyette@eeel.nist.gov

[‡] Electronic mail: wang@eeel.nist.gov

1. Introduction

Fluorinated compounds are extensively used in plasma processing applications in the microelectronics industry. Many of the fluorinated compounds used in plasma processing, however, have high global-warming potentials (GWPs), and the reduction of global-warming gas emissions from plasma processing is an issue of growing significance. One of several approaches to this problem being considered is to identify substitute plasma chemistries based upon gases having lower GWPs than those currently in use which are practicable for plasma processing applications [1, 2, 3]. Two such gases which have attracted particular interest are CF_3I and $\text{CF}_3\text{CH}_2\text{F}$ (HFC-134a). The etching properties of high density discharges sustained in each gas have been investigated in a number of recent studies.

The first examination of the effectiveness of etching by CF_3I discharges was by Karecki *et al.* [1] who evaluated the high-aspect-ratio etching performances and examined the effluent compositions from high density plasmas generated in CF_3I and other low GWP iodofluorocarbon and hydrofluorocarbon gases. Although other plasma chemistries were reported to demonstrate better etching properties, CF_3I discharges emitted the lowest levels of global-warming gases of the plasma chemistries they investigated. In a later study, Samukawa *et al.* [3] also studied dielectric etching in high density CF_3I discharges, measuring etch rates, selectivity, and relative CF_x radical densities. In their experiments, CF_3I discharges demonstrated selectivity comparable to and etch rates greater than those observed in C_2F_6 and *c*- C_4F_8 discharges. These observations were similar to those of Misra *et al.* [2], who observed $\text{CF}_3\text{I}/\text{O}_2$ rf discharges to etch SiO_2 and SiN films at rates comparable to conventional $\text{C}_2\text{F}_6/\text{O}_2$ mixtures.

HFC-134a, on the other hand, has emerged as a leading low GWP replacement for chlorofluorocarbon refrigerants [4]. The only reported investigation of etching with HFC-134a plasmas is that of Kirmse *et al.* [5]. Incidentally, they selected to study HFC-134a electron cyclotron discharges not for environmental reasons, but rather because of the high carbon-to-fluorine ratio of this molecule. Nevertheless, HFC-134a has a considerably shorter atmospheric lifetime, and lower GWP than many conventional plasma processing gases (see table 1). Pure HFC-134a discharges were observed to effectively remove SiO_2 without any etching of the underlying Si, leading Kirmse *et al.* [5] to report a remarkable infinite etching selectivity from these discharges.

The objective of this work is to examine the identities, fluxes, and energy distributions of ions produced in high density discharges generated in these two low GWP gases which have demonstrated promising etching properties. Positive ion bombardment plays an essential role in plasma etching, influencing etch rates, materials selectivity, and etching profiles. Experimental determination of ion identities and energies in processing plasmas provides complementary data necessary to validate the accuracy of plasma modelling efforts, and contributes to a fundamental understanding of the underlying discharge physics and chemistry relevant to processing applications. We present mass analysed ion energy distributions (IEDs), relative ion flux densities,

Table 1. Atmospheric lifetimes and 100 yr global-warming potentials of several fluorocarbon gases.

Gas	Atmospheric lifetime (yr)	GWP ₁₀₀	
CF ₄	50 000	6300	[28]
C ₂ F ₆	10 000	12 500	[28]
<i>c</i> -C ₄ F ₈	3200	9100	[28]
CHF ₃	250	12 100	[28]
CF ₃ I	<5×10 ⁻³	<1	[1]
HFC-134a (CF ₃ CH ₂ F)	14	1300	[28]

and absolute total ion currents in inductively coupled discharges sustained in CF₃I and HFC-134, as well as in various mixtures of each gas with Ar. These quantities were measured using a combined ion energy analyser-mass spectrometer that samples ions through an orifice in the lower electrode of a GEC rf reference cell.

2. Experiment

The discharges studied were generated in a GEC rf reference cell reactor whose upper electrode has been replaced with a five-turn planar rf-induction coil behind a quartz window to produce inductively coupled discharges [6]. The design of the GEC rf reference cell is described in detail elsewhere [7, 8]. A quartz annulus was mounted to the upper quartz window of the GEC cell. This ring was developed for use in the GEC rf reference cell to allow the generation of plasmas in electronegative gases over a much broader range of pressures and powers. The reactor, along with the ion energy analyser and mass spectrometer are depicted schematically in figure 1. The feed gas enters the cell through one of the 7 cm (2.75 in) side flanges and is pumped out through the 15 cm (6 in) port attached to the turbomolecular pump. The gas pressure is maintained by a variable gate valve between the GEC cell and the pump. Mass flow controllers regulated the gas flow, which was maintained at either 3.73 μmol/s (5 sccm) for pure CF₃I and HFC-134a discharges or 7.45 μmol/s (10 sccm) for mixtures of either CF₃I or HFC-134a with Ar.

A 13.56 MHz voltage is applied to the coil through a matching network. The rf power values presented in this article are the net power to the matching network driving the coil. The lower electrode is grounded to the vacuum chamber.

The ion sampling arrangement is identical to that used to study inductively coupled plasmas in other fluorocarbon gases [9, 10, 11], and in Ar, N₂, O₂, Cl₂, and their mixtures [12]. Ions are sampled through a 10 μm diameter orifice in a 2.5 μm thick nickel foil spot-welded into a small counterbore located at the center of the stainless steel lower electrode. For IED measurements, the ions that pass through the orifice are mass

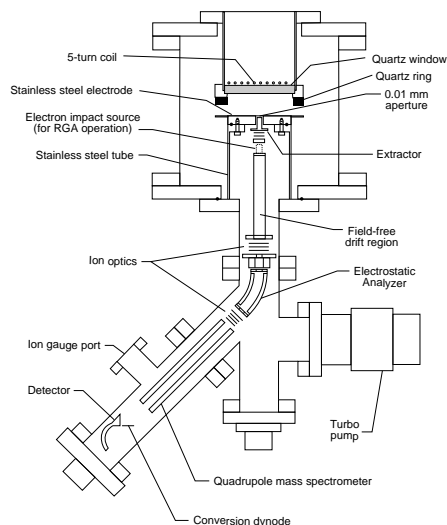


Figure 1. Schematic diagram of the inductively-coupled GEC rf reference cell reactor with the ion energy analyser and mass spectrometer appended to the modified lower electrode.

selected by the quadrupole mass spectrometer after being energy analysed by the 45° electrostatic energy selector. The IEDs measured in this manner are essentially ion-flux energy distributions [13].

Past experience with the ion energy analyser indicates that the ion transmission is nearly constant over the energy ranges observed here [13]. A mass-dependent transmission correction factor, however, was applied to the highest mass ions (mass > 40 u) in order to compensate for some decrease in the ion transmission of the quadrupole mass spectrometer with increasing mass. These factors were determined by calibration with rare gas plasmas [12] and approach a factor of 22 for I^+ at 127 u.

For total ion current measurements, (i.e. all ion current passing through the sampling orifice), the ion optic elements at the front of the ion energy analyser are biased such that the current passing through the sampling orifice is collected on the extractor element (the first ion optic element behind the electrode surface), and is measured using an electrometer. The total ion current (flux) measurements for plasmas with the same pressure, power, and gas compositions generally agreed to within 15%.

The total ion current is partitioned into mass channels according to the mass spectrum of ions. The absolute intensities of the measured IEDs are then determined by scaling the measured values of the ion current for the appropriate mass channel to the total ion current. The ion flux densities presented here are derived by dividing the

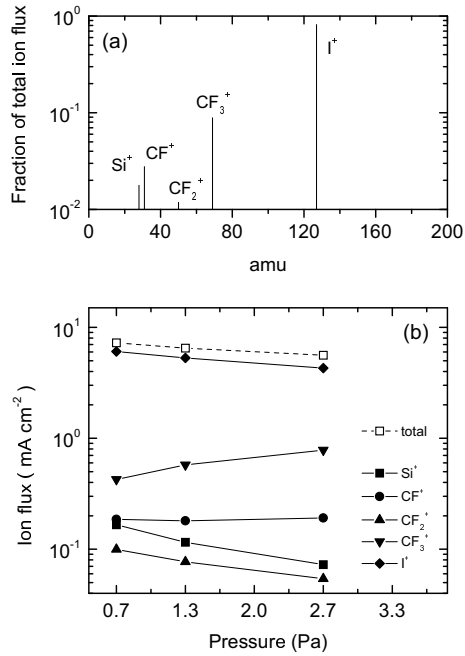


Figure 2. (a) Mass spectrum of ions striking the grounded electrode in an inductively coupled CF_3I discharge sustained at 1.33 Pa and 200 W, and (b) mass-resolved ion fluxes from CF_3I discharges at various pressures.

total measured ion current by the area of the $10\ \mu\text{m}$ diameter sampling hole.

3. Results and Discussion

3.1. CF_3I discharges

Figure 2(a) shows a mass spectrum of positive ions extracted from an inductively coupled CF_3I discharge which was operated at 1.33 Pa and 200 W. I^+ is by far the most abundant ion, comprising more than 80% of the observed ion current and is the heaviest ion observed. The cross section for electron-impact ionization of CF_3I to form CF_3I^+ is larger than the cross sections for any of the dissociative channels [14]. However, CF_3I^+ was not observed from these discharges, suggesting that electron-impact of CF_3I is not a major mechanism controlling the ion composition and that a large fraction of CF_3I may likely be dissociated in the plasma before ionization occurs. Moreover, reactions between CF_x^+ ($x = 1,2,3$) and CF_3I as well as between I^+ and CF_3I principally form CF_2I^+ as a reaction product [15, 16]. The similar absence of CF_2I^+ from the detected ion flux from CF_3I discharges is also consistent with a large fraction of CF_3I becoming dissociated through non-ionizing mechanisms.

In order to verify that our failure to detect CF_3I^+ was not caused by insufficient instrumental sensitivity to ions of such large mass, we observed the flux of neutral

species passing through the sampling orifice with and without a discharge present after filling the chamber with 1.33 Pa (10 mTorr) of CF_3I mixed with Ar. The instrument was then operated as a residual gas analyser, with the first ion optic element biased to exclude the flux of positive ions through the orifice, and neutral species entering the orifice were ionized using an internal electron source. Without a discharge present, a large flux of CF_3I^+ produced from CF_3I entering the orifice was observed. Once a discharge was initiated, however, the CF_3I^+ flux dropped substantially. Because the gas density decreases after the discharge is ignited due to an increase in gas temperature, the measured CF_3I^+ fluxes cannot be compared directly. Instead, the ratio of CF_3I^+ to Ar^+ flux was compared before and after discharge initiation to account for gas density variations. This ratio decreases approximately 90% after discharge initiation, indicating that nearly all of the CF_3I is dissociated within the plasma.

There are a number of processes which may be responsible for effectively dissociating CF_3I prior to ionization. The C-I bond energy is lower than the electron affinity of I, and dissociative electron attachment to CF_3I occurs rapidly and at thermal energies [17, 18, 19]. The experiments of Shimamori *et al.* [19] determined the rate constant for thermal dissociative electron attachment to CF_3I to be approximately $1.7 \times 10^{-7} \text{ cm}^3/\text{s}$, which is two orders of magnitude higher than the rate constants measured by Morris *et al.* [15, 16] for reactions between CF_3I and its fragment ions. Such high dissociative electron attachment rates likely contribute considerably to CF_3I dissociation in these discharges, although the subsequent neutralization of resultant I^- necessary prior to I^+ formation via electron impact would likely limit the overall rate of I^+ production resulting from this means of dissociation. The weak C-I bond makes it plausible that electron-impact dissociation of CF_3I into neutral fragments may also contribute to CF_3I dissociation, although the cross section for this process has not yet been measured. Ultraviolet photodissociation of CF_3I is another possible mechanism of CF_3I dissociation in these discharges [20]. The rate constant for thermal decomposition of CF_3I has been measured by Kumaran *et al.* [21] between 1000 K and 2100 K. Near 1000 K, the rate constant for this process is small, of the order $10^{-16} \text{ cm}^3 \text{ s}^{-1}$, suggesting that, although plausible, this process does not contribute significantly to CF_3I dissociation in these discharges. The availability of multiple dissociative mechanisms is likely responsible for the nearly complete dissociation of CF_3I that we observe in these plasmas.

The mass spectrum of ions in figure 2(a) is consistent with the assumption of a plasma gas that is almost completely dissociated into CF_3 radicals and I atoms. The cross section for electron-impact ionization of I is quite large (approaching 10^{-16} cm^2 near 13 eV) with a low threshold near 10.4 eV [22]. Ionization of the CF_3 radicals has a threshold also near 10 eV, with CF_3^+ being the dominant ionization product near threshold energies [23]. The cross sections for the ionization of CF_3^+ [24], however, are all significantly below those for the ionization of I. These differences, combined with the fact that dissociative recombination provides an efficient volume recombination mechanism for CF_3^+ and other polyatomic ions, may in part explain why I^+ is so dominant in CF_3I discharges.

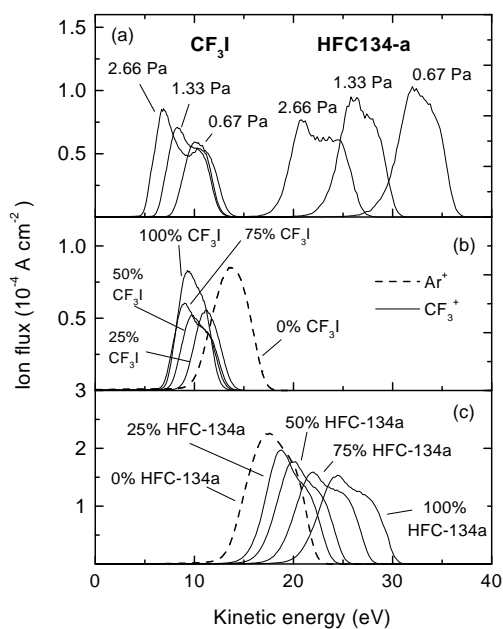


Figure 3. (a) Energy distributions of CF_3^+ ions (solid lines) in CF_3I and HFC-134a discharges as functions of pressure. Energy distributions of CF_3^+ and Ar^+ ions (dashed lines) in discharges containing different mixtures of (b) CF_3I and (c) HFC-134a with Ar . Discharges in (b) and (c) operated at 1.33 Pa and 200 W.

CF_3^+ is the second most abundant ion, comprising only about 9% of the ion yield. Although only a small fraction of the total ion current, CF_3^+ has a flux approximately 3 and 5 times larger than those of CF^+ and CF_2^+ respectively, making CF_3^+ the dominant CF_x^+ ion. The selective formation of CF_3^+ over other fluorocarbon ions agrees with the observations of Samukawa *et al.* [3]. Although Samukawa *et al.* [3] mention I^+ in passing, no data are presented regarding the quantities of I^+ observed in their ultrahigh frequency CF_3I discharges. The role of I^+ , if any, in plasma etching in CF_3I discharges is unclear. Ions containing Si or O which are produced from erosion of quartz surfaces within the cell total to only a few percent of the total ion current. This differs from previous studies of inductively coupled CHF_3 , C_2F_6 , and *c*- C_4F_8 plasmas generated in the same reactor in which significant quantities of such ions were detected [10, 11].

The mass-resolved ion fluxes in CF_3I discharges at different pressures are shown in figure 2(b). The total ion current and the fluxes of most significant ionic species decrease from 0.67 Pa to 2.66 Pa, with the exceptions of CF^+ and CF_3^+ : The CF^+ flux is nearly independent of pressure while the CF_3^+ flux nearly doubles in this range. The increase in CF_3^+ flux with pressure is suggestive of ion-molecule reactions contributing to CF_3^+ production. Figure 3(a) shows corresponding CF_3^+ energy distributions for these discharge conditions. At higher pressures, the IEDs show pronounced bimodal splitting

resulting from increased rf modulation of the ions' energy as they are accelerated across the plasma sheath [25, 26]. The increase of rf modulation with pressure can be attributed to a decrease in the ground sheath capacitance resulting from a more confined plasma as the pressure increases. The mean energies of these distributions, which correspond to the average plasma potentials of the discharges, decrease with increasing pressure. Changes in the ground sheath capacitance as well as reduced electron energies resulting from higher collisional frequencies contribute to this effect [27]. The energy distributions of the dominant ion I^+ and their dependence on discharge pressure closely resemble those of CF_3^+ .

It is interesting to note that the average plasma potentials in CF_3I discharges are considerably lower than those measured in inductively coupled discharges sustained in other fluorocarbon gases we have studied [9, 10, 11], including those with the same carbon to fluorine ratio (CHF_3) [10], or with similar molecular weight (*c*- C_4F_8) [11]. Average plasma potentials in CF_3I discharges are lower than those observed in Ar under similar conditions [12]. Samukawa *et al.* [3] postulated that high ionization rates in their CF_3I discharges produced the high plasma densities and low electron temperatures that they measured. The ionization potentials of the dissociation fragments I and CF_3 are lower than the ionization potentials or dissociative ionization thresholds of other fluorocarbon gases we have studied. With nearly complete dissociation of CF_3I in the plasma and the low ionization potentials of the resulting fragments, it is possible that ionization occurs more effectively in CF_3I discharges.

Figure 4(a) and Figure 3 (b) show the mass-resolved flux of positive ions extracted from discharges generated in different mixtures of CF_3I and Ar and the CF_3^+ energy distributions in these discharges, respectively. The total ion current and the Ar^+ current change considerably between 0% and 25% CF_3I by volume. While the total ion yield decreases nearly 35%, the Ar^+ flux drops by more than an order of magnitude in this range. Beginning with a 75% Ar mixture, Ar^+ drops to <10% of the ion current and I^+ instead dominates with nearly 70% of the total ion yield. As the CF_3I fraction is raised further, the flux of Ar^+ continues to decline sharply, decreasing more rapidly than does the proportion of Ar in the feed gas mixture, while the flux of I^+ remains nearly constant. The average plasma potential as indicated by the CF_3^+ energy distributions decreases between 0% and 25% CF_3I by volume, although the effect of further CF_3I addition to the average plasma potential is small. The CF_3^+ flux intensity is the highest of the fluorocarbon ions detected and approximates the increase in CF_3I fraction. The intensities of ions produced from erosion of quartz surfaces are small and decrease by nearly a factor of four between 25% and 100% CF_3I .

3.2. HFC-134a

Figure 5(a) shows a mass spectrum of positive ions extracted from an inductively coupled HFC-134a discharge operated at 1.33 Pa and 200 W. Several ions of significant intensity are detected, with HF^+ and Si^+ the most abundant. In addition to fluorocarbon ions,

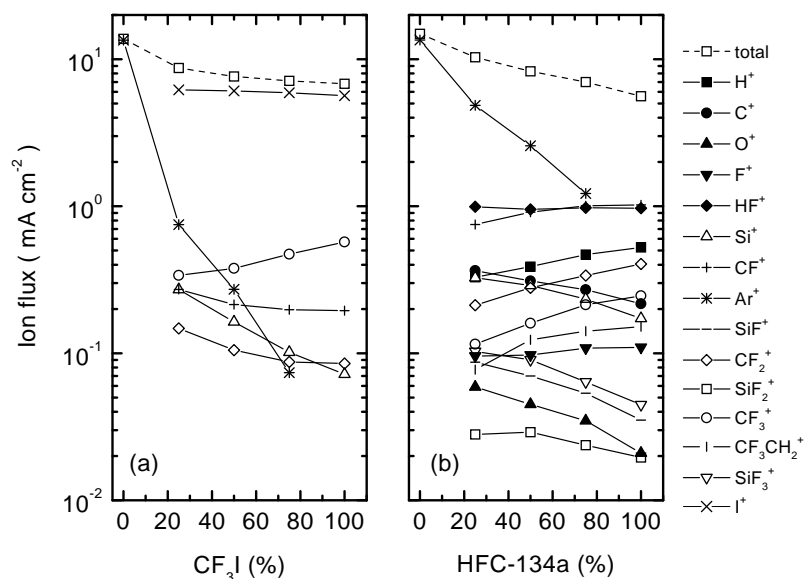


Figure 4. Mass analysed ion fluxes in discharges containing (a) CF_3I and (b) HFC-134a for various mixtures with Ar. All discharges operated at 1.33 Pa and 200 W.

H^+ and SiF_x^+ species had significant fluxes as well. The presence of hydrogen in these discharges prevents analysis of the relative abundances of Si isotopes to distinguish SiF_x^+ species from COF_x^+ species. The presence of a moderate flux of O^+ from these discharges, however, suggests that a fraction of flux attributed to SiF_x^+ species may possibly consist of COF_x^+ species instead. It is interesting to note that CF^+ constitutes a majority of the CF_x^+ ion flux. The relative fluxes of ions at the substrate position in HFC-134a electron cyclotron resonance discharges were measured by Kirmse *et al.* [5]

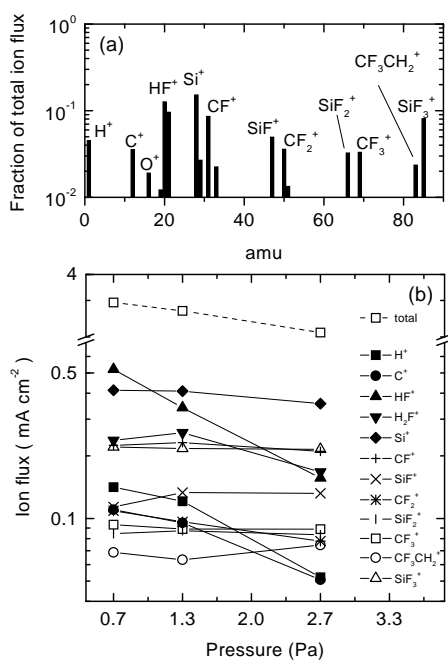


Figure 5. (a) Mass spectrum of ions striking the grounded electrode from a 1.33 Pa, HFC-134a inductively coupled discharge sustained at 200 W and (b) mass-resolved ion fluxes from HFC-134a discharges as functions of pressure.

as O_2 was incrementally added to the feed gas. Although they did not report the relative abundances of the ionic species, several ionic species which they detected were observed in our inductively coupled HFC-134a discharges. Exceptions are H^+ and $CF_3CH_2^+$, both of which we observed in significant quantities, but are not listed by Kirmse *et al.* [5].

The mass-resolved ion fluxes and CF_3^+ energy distributions in HFC-134a discharges at different pressures are shown in Figure 5(b) and Figure 3(a), respectively. With the exception of Si^+ , the fluxes of atomic ions and HF^+ are the most sensitive to discharge pressure, whereas the intensities of all other significant ions remain fairly constant. As was the case in CF_3I discharges, the total ion current and the mean ion energies both decrease at higher discharge pressures, suggesting reduced electron energies at higher collisional frequencies. Unlike in CF_3I discharges, the flux of CF_3^+ in HFC-134a discharges is fairly insensitive to discharge pressure. The average plasma potentials in HFC-134a discharges decrease from 27 eV to 22 eV from 0.67 Pa to 2.66 Pa, a greater absolute and relative decrease in average plasma potential than those observed in CF_3I discharges.

Figure 4(b) shows the mass-resolved flux of positive ions extracted from discharges sustained in different mixtures of HFC-134a and Ar. The Ar^+ flux decreases in proportion to its reduced concentration in the feed gas mixture while the CF_x^+ and $CF_3CH_2^+$ flux intensities grow with higher HFC-134a fractions. As with CF_3I discharges,

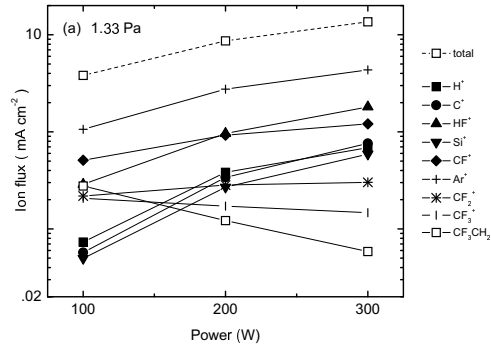
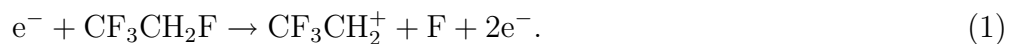


Figure 6. Mass analysed ion fluxes in 50% Ar : 50% HFC-134a discharges at various discharge powers.

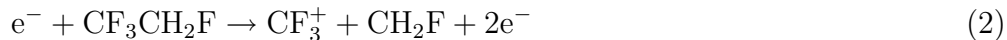
the intensities of SiF_x^+ ions decrease with higher HFC-134a fractions. Although the flux of H^+ rises with HFC-134a fraction, the fluxes of HF^+ and F^+ display little dependence on the HFC-134a fraction. CF_3^+ energy distributions corresponding to these plasma conditions are shown in figure 3(c). Average plasma potentials progressively decrease from 27 eV to 18 eV and the distributions narrow with the gradual addition of Ar. The reader may notice in figure 3 the mean ion energies in 0% CF_3I and 0% HFC-134a discharges differ by approximately 3 eV although these distributions correspond to ostensibly identical plasma operating conditions (i.e. 100% Ar discharges). The mean ion energy in 0% HFC-134a discharges agrees with measurements made by Wang *et al.* [12] made in inductively coupled Ar plasmas in the same GEC reference cell. It is likely that residual species remaining in the cell after CF_3I discharges were run provided a source of contamination for “pure” Ar discharges run afterwards.

Figure 6 shows the dependence of several significant ions in 50% Ar : 50% HFC-134a discharges on discharge power. The intensity of CF_3CH_2^+ decreases by more than a factor of four between 100 W and 300 W. Although little is known regarding electron interactions with HFC-134a, CF_3CH_2^+ very likely is produced from dissociative ionization of HFC-134a:



The decrease in CF_3CH_2^+ flux at higher powers is consistent with a reduced HFC-134a

density at higher discharge powers, indicating that the HFC-134a dissociation fraction increases with discharge power. This is further supported by the observation that the fluxes of other ions likely to be formed mainly via dissociative ionization of HFC-134a such as CH_2F^+ and CF_3CHF^+ (data not shown) also decrease with higher discharge powers. The CF_3^+ flux decreases slightly from 100 W to 300 W, suggesting that another possible dissociative ionization channel of HFC-134a



accounts for a significant fraction of CF_3^+ production in these discharges.

4. Summary

We have determined the identities, fluxes, and energy distributions of ions produced in high density discharges generated in two low GWP gases, CF_3I and $\text{CF}_3\text{CH}_2\text{F}$ (HFC-134a), which have been reported to demonstrate desirable plasma processing characteristics. The effects of plasma operating conditions as well as the dilution of each gas with Ar on ion fluxes and energies were examined. I^+ comprises nearly all of the ion yield in CF_3I discharges, and high rates of dissociative electron attachment contribute to nearly complete dissociation of CF_3I in these discharges. Mean ion energies are low, ranging from 5 eV to 10 eV over the range of operating conditions investigated. Discharges generated in mixtures of CF_3I and Ar have ion fluxes and energies resembling those of pure CF_3I discharges. Discharges generated in HFC-134a, on the other hand, produce several ions of significant intensity, with HF^+ and Si^+ being the most abundant. Mean ion energies in HFC-134a discharges are considerably higher, ranging from 20 eV to 35 eV, and decrease as HFC-134a is diluted with Ar. Increasing the discharge power results in greater dissociation in HFC-134a discharges, shifting the reactive ion composition towards higher fluxes of lighter ions.

Acknowledgments

One of the authors (ANG) gratefully acknowledges the support of a National Research Council postdoctoral associateship.

References

- [1] Karecki S, Pruette L, Reif R, Sparks T, Beu L and Vartanian V 1998 *J. Electrochem. Soc.* **145** 4305
- [2] Misra A, Sees J, Hall L, Levy R A, Zaitsev V B, Aryusook K, Ravidranath C, Sigal V, Kesari S and Rufin D 1998 *Mater. Lett.* **34** 415
- [3] Samukawa S, Mukai T and Tsuda K 1999 *J. Vac. Sci. Technol. A* **17** 1
- [4] Morrison G and Ward D K 1991 *Fluid Phase Equilibria* **62** 65
- [5] Kirmse K H R, Wendt A E, Disch S B, Wu J Z, Abraham I C, Meyer J A, Breun R A and Woods R C 1996 *J. Vac. Sci. Technol. B* **14** 710
- [6] Miller P A, Hebner G A, Greenberg K E, Pochan P S and Aragon B P 1995 *J. Res. Natl. Inst. Stand. Technol.* **100** 427
- [7] Hargis P J *et al.* 1994 *Rev. Sci. Instrum.* **65** 140
- [8] Olthoff J K and Greenberg K E 1995 *J. Res. Natl. Inst. Stand. Technol.* **100** 327
- [9] Olthoff J K and Wang Y 1999 *J. Vac. Sci. Technol. A* **17** 1552
- [10] Wang Y, Misakian M, Goyette A N and Olthoff J K *J. Appl. Phys.* submitted
- [11] Goyette A N, Wang Y, Misakian M and Olthoff J K *J. Vac. Sci. Technol. A* submitted
- [12] Wang Y and Olthoff J K 1999 *J. Appl. Phys.* **85** 6358
- [13] Rao M V V, Van Brunt R J and Olthoff J K 1996 *Phys. Rev. E*, **54** 5491
- [14] Jiao C Q unpublished
- [15] Morris R A, van Doren J M, Viggiano A A and Paulson J F 1992 *J. Chem. Phys.* **97** 173
- [16] Morris R A, Viggiano A A, van Doren J M and Paulson J F 1992 *J. Phys. Chem.* **96** 2597
- [17] Heni M and Illenberger E 1986 *Chem. Phys. Lett.* **131** 314
- [18] Hahndorf I and Illenberger E 1997 *Int. J. Mass Spectrom.* **167** 87
- [19] Shimamori H and Nakatani Y 1988 *Chem. Phys. Lett.* **150** 109
- [20] Rattigan O V, Shallcross D E and Cox R A 1997 *J. Chem. Soc. Faraday Trans.* **93** 2839
- [21] Kumaran S S, Su M C, Lim K P and Michael J V 1995 *Chem. Phys. Lett.* **243** 59
- [22] Hayes T R, Wetzel R C and Freund R S 1987 *Phys. Rev. A* **35** 578
- [23] Christophorou L G, Olthoff J K and Rao M V V S 1996 *J. Phys. Chem. Ref. Data* **25** 1341
- [24] Deutsch H, Märk T D, Tarnovsky V, Becker K, Cornelissen C, Cespiva L and Bonacic-Koutecky V 1994 *Int. J. Mass Spectrom.* **137** 77
- [25] Hopwood J 1993 *Appl. Phys. Lett.* **62** 940
- [26] Gudmundsson J T 1999 *Plasma Sources Sci. Technol.* **8** 58
- [27] Wang Y 1994 *Appl. Phys. Lett.* **66** 2186
- [28] Houghton J T, Meira Filho L G, Bruce J, Lee H, Callander B A, Haites E, Harris N and Maskell K 1995 *Climate change, 1994 : radiative forcing of climate change and an evaluation of the IPCC IS92 emission scenarios* (New York: Cambridge University Press) p 33